Available online at www.sciencedirect.com

ScienceDirect

journal homepage: www.elsevier.com/locate/he

From the can to the tank: $NaAlH_4$ from recycled aluminum

R. Guerrero-Ortiz, J.R. Tena-García, A. Flores-Jacobo, K. Suárez-Alcántara*

Unidad Morelia del Instituto de Investigaciones en Materiales de la Universidad Nacional Autónoma de México, Antigua Carretera a Pátzcuaro No. 8701, Col. Ex Hacienda de San José de la Huerta, C.P. 58190, Morelia, Michoacán, Mexico

HIGHLIGHTS

- We use Al from recycling Al-cans to produce $NaAlH_4$ as a hydrogen storage material.
- Flakes of Al-cans and NaH (plus additives) were ball milled.
- $NaAlH_4$ produced by this method is competitive with pure-precursor material.

GRAPHICAL ABSTRACT

(a) (b) (c)

ARTICLE INFO

Article history:
Received 25 March 2019
Received in revised form
3 June 2019
Accepted 5 June 2019
Available online 3 July 2019

Keywords:
Hydrogen storage
Recycled Al
Sodium alanate

ABSTRACT

The recycling of Al-cans (from soft beverages cans) by a ball milling process and its use as a main component of a hydrogen storage material is presented. The recycled Al, together with NaH, TiF_3 as the catalyst, and C-nanotubes as milling agent were milled together as precursors of $NaAlH_4$. The material presented a reversible hydrogen storage capacity of 3.7 wt% at 150 °C and up to 100 bar hydrogen pressure. Characterization of the as-milled and hydrogenated materials indicates the feasibility of using Al recycled for producing $NaAlH_4$.

Introduction

The search for renewable and efficient energy sources is one focus of attention in materials science today. Hydrogen steps ahead as one of the most promising alternative fuel and recent research focus on its storage and performance in optimal conditions for mobile applications in the years to come [1–3]. The main goal of any research in hydrogen storage is to develop materials with high storage capacity, good

* *Corresponding author.*
E-mail address: karina_suarez@iim.unam.mx (K. Suárez-Alcántara).
https://doi.org/10.1016/j.ijhydene.2019.06.033

performance, reversibility, and rapid reaction kinetics. Sodium alanate ($NaAlH_4$) is one of the most studied materials due to its potential as a hydrogen storage medium. Bogdanović et al. demonstrate the reversible hydrogen storage/release in sodium alanate by doping with Ti compounds, according to reactions [4]:

$$NaAlH_4 \leftrightarrow 1/3\ Na_3AlH_6 + 2/3\ Al + H_2 \quad (1)$$

$$1/3\ Na_3AlH_6 \leftrightarrow NaH + 1/3\ Al + ½\ H_2 \quad (2)$$

Reactions (1) and (2) sum a reversible storage capacity of 5.6 wt%. Dehydrogenation reactions are performed between 100 and 280 °C and low pressure. Meanwhile, hydrogenation is performed at pressures as high as 130 bar and temperatures around 100–150 °C [5,6]. This hydrogenation/dehydrogenation temperatures are in the border-line of compatibility with high-temperature proton exchange polymer fuel cells (PEMFC) [7]. Cycling studies have demonstrated stability over 100 cycles [8]. Further improvements are expected by the use of scaffolds or other supports that have a strong influence in hydrogenation/dehydrogenation kinetics [9–11]. Despite the good perspectives of the $NaAlH_4$ as reversible hydrogen storage material, the $NaAlH_4$ is not massively used. One of the reasons for that is the high cost of $NaAlH_4$. In turn, the high cost of $NaAlH_4$ is due to the difficulty and danger of its syntheses in organic solvents. Commercially, $NaAlH_4$ is produced in organic solvents (toluene, hexane, n-octane, ether, THF, etc.) from Na o NaH, an excess of Al (up to 3:1), Ti-catalyst, and H_2 [12]. The mixture of organic solvents, NaH and Al with oxygen/humidity is highly explosive. This production method needs steps of purification and drying. Because of that, the $NaAlH_4$ is frequently sold in THF solution. The development of the $NaAlH_4$ synthesis by means of mechanical milling of NaH and Al and posterior hydrogenation eliminated the need for organic solvents, purification and drying steps [13,14]. However, this method is usually performed only in lab-scale for studies of hydrogen storage.

Other important points, not frequently discussed, are the sustainability and availability of raw materials. High-purity raw materials for $NaAlH_4$ syntheses had been customarily used and reported; yet these materials are not always available, predominantly in developing countries. On the other hand, the use of high-purity raw materials is adequate for research purposes [15,16]. However, this can lead to high costs of manufacture if massive production would be intended. To the best of the author's knowledge just Bergemann et al. have studied the possibility of producing sodium alanate by reactive ball-milling of particles obtained from recycled Al-slags (from waste and incinerated) [17].

In the present work, we propose the use of Al from recycled beverage cans to produce $NaAlH_4$ as a hydrogen storage material without the energy expenses that involves the incineration. The main reasons and/or advantages for this are:

i) The recycling of solid residues such as Al cans can be incentivized by the production of sustainable $NaAlH_4$.
ii) Reduce the energy of recycling Al for $NaAlH_4$ production: Aluminum is usually recycled by means of the melting of waste materials, included the $NaAlH_4$ production [17]. That is a method of high-temperature that necessarily implies high-energy consumption, not recommend if the reduction of energy consumption is desired in an industrial process [18]. The present work uses one step of mechanical milling to produce a precursor mixture for $NaAlH_4$ production.
ii) The cost of producing a material for hydrogen storage such as $NaAlH_4$ could be reduced by the recycling of Al beverage cans; while the quality could be not severely compromised. The Al beverage cans are usually manufactured with the 6061 Al-alloy [19]. The chemical composition of 6061 Al-alloy (minimum and maximum) is indicated in Table 1. Thus, the Al from beverage cans could be a good-quality source of Al, of low-cost, for hydrogen storage purposes. Additionally, the alloying elements can be beneficial for hydrogen storage. For example, Mg is a hydrogen storage material by itself; meanwhile, Fe, Cu, Zn, and Ti had been widely used as accelerators for hydrogenation/dehydrogenation reactions.
iii) The purchasing of high-purity and fine-grinded metals or metal-hydrides powders of Al, Ti or Mg is facing increasing restrictions in certain developing countries.

Materials and methods

Al-cans conditioning and mixture preparation

Aluminum beverage cans were collected at the university campus and used without severe washing, just a slight washing to avoid an excessive presence of dust or organic waste materials (sugars). The labeling (polymers and inks) of the cans was not removed, thus that materials were also milled. Both conditions were used to keep circumstances close to an industrial process. To guarantee the same components of Al-alloy, only a brand, and a type of cans was used (regular *coca-cola*). The beverage cans were cut manually into approximately 0.25 cm^2 flakes (approx. 0.5 cm per side). Due to the manually cutting with scissors, only the bodies of the cans were used, the tops and bottoms were discarded. Perhaps in an industrial process, all the parts of the cans could be recycled by using an automatized cutter.

In a first milling approach, only Al-flakes were milled while a visual inspection allowed the determination of

Table 1 – Chemical composition of 6061 Al-alloy [19], and EDS[a] experimental results of Al-cans.

Element	Minimum (wt. %)	Maximum (wt. %)	Content[b] (wt. %), EDS
Al	96.0	98.61	87.5
Si	0.40	0.80	0.90
Fe	0.00	0.70	0.60
Cu	0.15	0.40	0.60
Mn	0.00	0.15	0.90
Mg	0.80	1.20	0.90
Cr	0.04	0.35	–
Zn	0.00	0.25	–
Ti	0.00	0.15	8.60

[a] Energy-dispersive X-ray spectroscopy.
[b] Experimental results.

optimal milling time. The depletion of Al-flakes happened after 10 h of milling. This stage was performed to understand the milling of Al-flakes. After that, a mixture of Al-flakes, NaH, TiF_3, and carbon nanotubes (Al_{cans}/NaH/TiF_3/C-nanotubes hereafter) was milled together, establishing a single milling procedure of 15 h. The TiF_3 was used as an accelerator of the hydrogenation/dehydrogenation reactions while the carbon nanotubes were used as a milling agent. Ce and La-compounds [20,21], or other Ti-compounds have a better performance as hydrogenation/dehydrogenation accelerators; however, the purchase of some these compounds is not easy in some developing countries. The strong tendency of Al to the sintering instead of milling (refinement of grain and crystal size) should be mentioned [22]. Thus, carbon nanotubes were used as the milling agent to avoid agglomeration of materials at the wall of the milling vial. The addition of carbon nanotubes also is well-known for improving the hydrogenation/dehydrogenation properties of the $NaAlH_4$ system [23,24].

Besides Al from cans, the rest of materials were: NaH, 95% purity, Aldrich; TiF_3, 99.995% purity, Aldrich; and carbon nanotubes, single-wall nanotubes, 99% purity, Aldrich. TiF_3 was added in a proportion of 5 wt %, while the carbon nanotubes were added in a proportion of 1 wt % of the total Al/NaH powder mixture. A 10 wt % excess of Al was used. The ball-milling was performed in a 316 L stainless steel milling vial of inner volume of 100 ml. The handling of materials was performed in a glovebox with high purity Argon (10 ppm of O_2 and H_2O). The milling vial was closed in Argon atmosphere and transferred to the mill outside the glove box. The design of the milling vial (bolted lid and Viton® seals) allowed appropriate sealing and avoided oxygen and moisture contamination during milling outside the glove-box. The milling balls were made of yttrium-stabilized zirconium oxide (1 cm diameter). The ball to powder ratio was 15:1. The milling was performed in a PQ-N04 Ball Mill planetary mill with 4 spots for vials (Across-International) with the rotation frequency of the main wheel of 40 Hz. The total milling time was 15 h divided into periods of 1-h milling and 10 min resting. In each cycle of milling-pause, the direction of the rotation of the planetary mill was inverted. The milled materials were recovered and stored in argon until further use.

Materials characterization

The as-milled and hydrogenated samples were characterized as necessary by scanning electron microscopy (SEM) including energy-dispersive X-ray spectroscopy (EDS), X-ray diffraction (XRD), and Fourier transformed infrared spectroscopy (FT-IR). SEM images were obtained in a JSM-IT300 microscope. Samples were dispersed on carbon tape inside the argon glove box. Then, they were transferred to the SEM chamber reducing the oxygen contact by means of a glove bag, even though partial oxidation could be possible. Unless otherwise indicated, SEM images were obtained by back-scattered or secondary electrons, and 10 kV or 20 kV of acceleration voltage. The range of conditions and detector were dictated by each sample accordingly its characteristics. X-ray diffraction experimentation was performed in a Bruker D2Phaser diffractometer (Cu Kα = 1.540598 Å). The powders of as-milled, and hydrogenated materials were compacted in a dedicated sample holder, then they were covered with Kapton foil for protection against ambient oxygen, and moisture during transfer to the diffractometer and data collection. FT-IR characterization was performed in a Nicolet iS10 of Thermo Fisher Scientific in ATR (Attenuated Total Reflection) mode. The studied materials were compacted in KBr pellets. The KBr was purchased from Sigma-Aldrich and dried just before the pellet preparation. About 2.5 mg of each material was dispersed in 50 mg of dry KBr.

Pressure-composition isotherms (PCI)

Pressure-composition isotherms were performed in an isorb-100 machine (Quantachrome). A sample of about 1 g of as-milled Al_{cans}/NaH/TiF_3/C-nanotubes was transferred to the machine without oxygen contact by means of a sample holder with an isolation valve. Then, the sample was heated at 150 °C under a dynamic vacuum for 12 h. This step was fundamental and we classify it as the activation of the sample. After this, the sample was cooled down and the calibration for void volume with ultrahigh purity helium was performed. Hydrogenation reactions were performed by a progressive increase (steps) of the hydrogen pressure from 0.1 to 100 bar. Dehydrogenation reactions were performed by a progressive decrease (steps) of the hydrogen pressure from 100 to 0.1 bar. The equilibrium conditions directed the time employed at each step. The equilibrium conditions were no-changes in the registered pressure superior to 0.1 mbar during 250 s, or a maximum time of 240 min per step. The cycles were recorded at 100, 150, and 200 °C. The hydrogen used during experiments was of chromatographic purity.

Temperature programmed desorption/sorption (TPD/TPS)

Temperature programmed dehydrogenation experiments were carried out in a Sieverts type apparatus of own design and construction [25]. Calibration and operation were performed as detailed in ref. [25]. Samples were transferred to the Sieverts-type reactor without oxygen contact by means of a closing valve at the sample holder. Then, the sample was heated at 150 °C under a dynamic vacuum for 12 h for activation. The hydrogenation was performed at 60 bar hydrogen pressure and at 100, 150, and 200 °C. The first step was to fix the initial pressure in the apparatus (60 bar), then the sample was heated at the test temperature with a heating ramp of 5 °C/min. The total hydrogenation time was 1 h, counted since the starting of the heating. Then, the sample was cooled down. At room temperature, the pressure was released. For dehydrogenation reactions, the initial pressure was fixed at 1 bar. After that, the oven temperature was raised from room temperature to 100, 150 and 200 °C with a heating rate of 5 °C/min. The total dehydrogenation time was 1 h, counted since the starting of temperature increase. After reactions, the system was cooled down and then purged for remaining hydrogen. The hydrogen used during experiments was of chromatographic purity.

Results

Visual inspection and characterization of the milling procedure

The Graphical Abstract present pictures of the Al recycling process, from the can to the obtaining of Al-powders. EDS (K series) report of the composition of the Al-flakes is presented in the last column of Table 1. EDS demonstrated that the content of Si, Fe, Cu, and Mn are slightly above the specifications of a 6061 alloy, and that the Ti content is very high respect specifications (Table 1). The Fe content indicates no contamination from milling vial. Cr and Zn were not detected.

In a first approach of milling, every hour, the milling vial was opened and we observed the relative amount of Al-flakes. 10 h was enough to mill all Al-flakes of about 0.25 cm^2. Then, the same procedure was performed for the Al_{cans}/NaH/TiF_3/C-nanotubes mixture. Here, the depletion of all the Al-flakes was reached in 15 h. The increase of the milling time was induced by a reduction of the effectiveness of ball-milling, particularly by the use of carbon particles that reduce the friction among particles. The milling was repeated several times to confirm the depletion of the Al-flakes. Then, the Al_{cans}/NaH/TiF_3/C-nanotubes mixture was characterized by XRD and SEM (Fig. 1). SEM image (Fig. 1a) demonstrated that the Al-flakes were reduced to particles of between 5 and 50 μm of diameter. The majority of particles are in the upper limit, i. e. 50 μm, which is very near to a −325 mesh size. Bright spots in SEM image (Fig. 1b) of the as-milled Al_{cans}/NaH/TiF_3/C-nanotubes correspond to Al-rich zones. The same conclusion about the Al-rich zones was obtained before in other studies [26]. In general, the TiF_3 is well dispersed. Thus, the milling time and conditions are adequate to transform Al-flakes to Al-micro and nanoparticles.

Fig. 1c presents the Al-flakes, as-milled Al_{cans}, and Al_{cans}/NaH/TiF_3/C-nanotubes mixture X-ray diffraction pattern. The Al-flakes presented a marked preferential orientation due to the process to produce the cans. The peak due to (220) plane reflections is more intense than the expected (111) reflections. The Al-flakes presented small peaks that coincide with carbon; this can be explained by the labeling (polymer and inks) of the can. Ball-milling changes the Al stresses and microstrains; the peaks intensity of as-milled Al_{cans} are the expected accordingly to crystallographic data (ICSD-43423). As-milled Al_{cans} indicate a refinement of the crystal size as compared with the original Al-flakes. The crystal size of as-milled Al_{cans} was determined by Rietveld analysis as 49.5 ± 0.4 nm. Meanwhile the crystal size of NaH and Al in the as-milled Al_{cans}/NaH/TiF_3/C-nanotubes sample were 18.2 ± 2.1 nm and 76.1 ± 3.8 nm, respectively. No indication of the rest of the components of the 6061 Al-alloy was found. The reduction of the effectiveness of the ball milling with the incorporation of NaH was confirmed by visual inspection and XRD results.

Hydrogenation and dehydrogenation reactions, PCI and TPD/TPS curves

Fig. 2a presents the phase diagram of the Ti-catalyzed system NaH + Al, Na_3AlH_6 and $NaAlH_6$ [27]. The pink lines and black squares indicate the path and maximum pressure during PCI

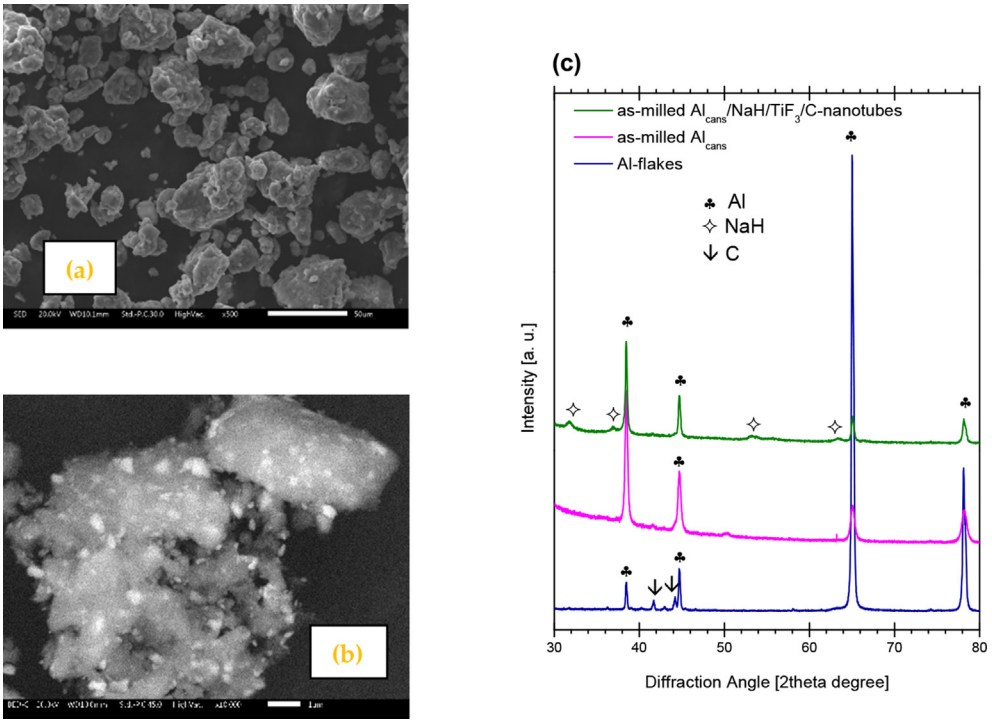

Fig. 1 – SEM and XRD characterization of as-milled Al_{cans} and Al_{cans}/NaH/TiF_3/C-nanotubes mixture. (a) SEM of as-milled Al_{cans} powder. (b) as-milled Al_{cans}/NaH/TiF_3/C-nanotubes mixture. (c) XRD of Al-flakes (Al_{cans} not-milled), as-milled Al_{cans}, and as-milled Al_{cans}/NaH/TiF_3/C-nanotubes mixture.

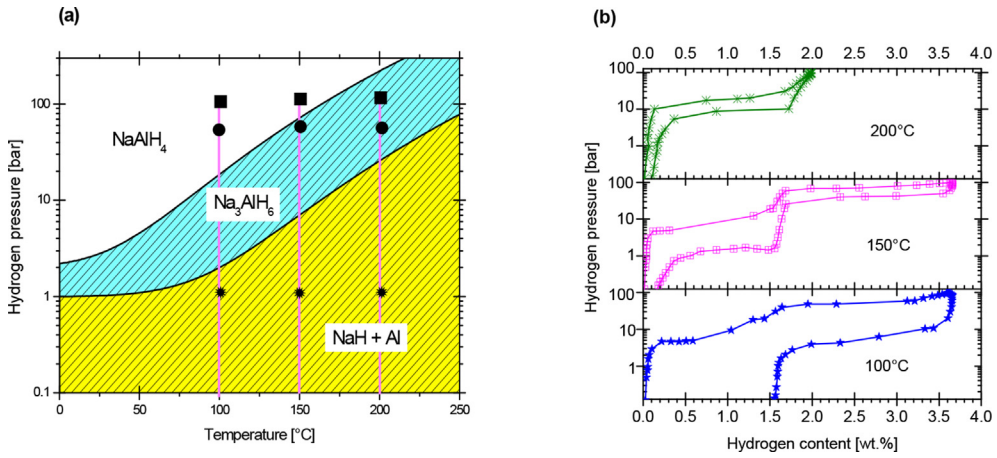

Fig. 2 – (a) Phase diagram of Ti-doped ($Ti(OBu)_4$) $NaAlH_4$, Na_3AlH_6 and NaH + Al [4,27,32]. (b) PCI curves of Al_{cans}/NaH/TiF_3/C-nanotubes mixture at different conditions of *p* and T.

experimentation, respectively. The dots and stars in Fig. 2a indicates the conditions used for temperature programmed desorption/sorption experiments. On the other hand, in our recycled material, the maximum expected capacity of hydrogen storage through the formation of $NaAlH_4$ is 3.99 wt% considering the 87.5 wt% purity of Al_{cans}, 95 wt% purity of NaH, The 10% excess of Al_{cans}, the 5 wt% of TiF_3 and the 1% of C-nanotubes. Fig. 2b presents the PCI curves of the Al_{cans}/NaH/TiF_3/C-nanotubes mixture. The results are consistent with the expected hydrogen content and the phase diagram. At 100 °C and 100 bar, the system is in the $NaAlH_4$ zone, the hydrogen uptake is 3.7 wt%. Meanwhile, at 200 °C and 100 bar, the system is in the Na_3AlH_6 zone, the hydrogen uptake is 2.0 wt%. Thus, hydrogenation would be more effective at 100 °C and 100 bar, not taking in account kinetic effects. However, at 100 °C dehydrogenation is not completed, the equilibrium plateau of the Na_3AlH_6/NaH + Al is not defined. The best conditions for hydrogenation and dehydrogenation reactions are defined by the PCI curve at 150 °C; the equilibrium plateaus are well-defined and the reactions can be considered as reversible. The PCI curves demonstrated that the material produced by the recycling of Al from cans meet the expected phase changes for a NaH + Al, Na_3AlH_6 and $NaAlH_6$ system.

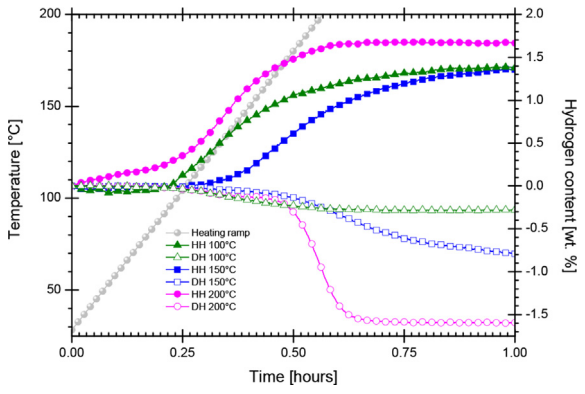

Fig. 3 – TPD and TPS curves at 60 bar and 1 bar, respectively, and 100, 150 and 200 °C. (HH = hydrogenation reaction, DH = dehydrogenation reaction).

Fig. 3 presents the TPD and TPS curves at 60 bar and 1 bar pressure, respectively, and 100, 150 and 200 °C temperature. It would be mentioned that our Sieverts type machine used for this experiments is limited to 60 bar hydrogen pressure as a maximum. Under this condition, only the formation of Na_3AlH_6 was expected. Normally the experiments of hydrogenation of NaH/Al/additives mixtures are carried out at pressures superior to 100 bar to form $NaAlH_4$ [28]. Even this circumstance, the Al_{cans}/NaH/TiF_3/C-nanotubes mixture presents a reversible hydrogen storage of 1.6 wt%. at 200 °C. The dehydrogenation at 150 and 100 °C is very limited at 1 bar hydrogen pressure. At 150 °C, the equilibrium pressure is about 1 bar (Fig. 2b). Some reports use very low pressures or vacuum to induce dehydrogenation at considerable rates [29]. The need for using very low or vacuum pressures for complete dehydrogenation is frequently considered as a drawback for the use of $NaAlH_4$ as a hydrogen storage material. However, the main objective of this work was the recycling of Al and its use as a precursor of a hydrogen storage material, not entirely the optimization of the material for kinetics. As mentioned in the introductory section, other additives than TiF_3 are more effective in accelerating the hydrogenation/dehydrogenation reactions, but they are not always available. Thus, in further research, a better catalyst can be used.

Characterization of the hydrogenated materials

Fig. 4a presents the SEM image of the hydrogenated material at 150 °C and 100 bar. This image is representative of the hydrogenated materials. The other hydrogenated materials did not show significant changes as compared with this image. The first observation is that the hydrogenated materials presented a huge agglomeration as compared with the as-milled materials. The agglomerate size is above 100 μm. This is consistent with the sintering of materials after exposing to high pressure and heating. Superficially, the particles have protuberances that the as-milled materials did not present.

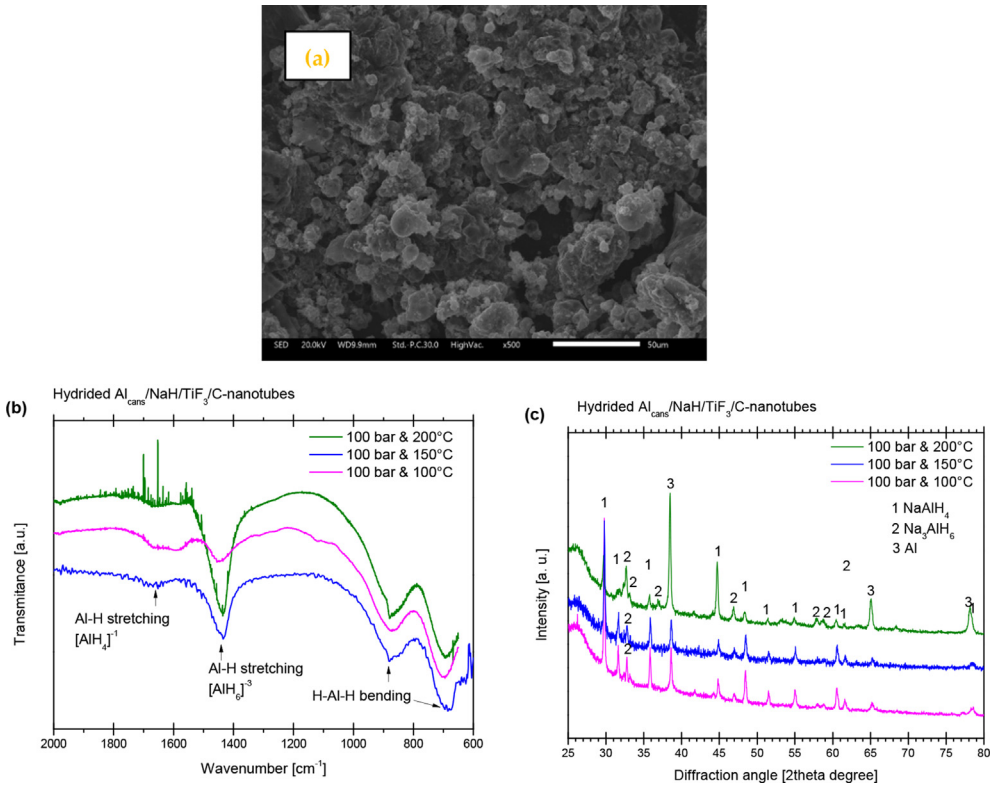

Fig. 4 – Characterization of hydrided materials. (a) SEM image. (b) FT-IR spectra. (c) X-ray diffraction patterns.

The protuberances can be associated with nucleation and grow sites of the hydrogenated compounds.

In the alanates, the common structures are the tetrahedral $[AlH_4]^{-1}$ and octahedral $[AlH_6]^{-3}$ units. The tetrahedral $[AlH_4]^{-1}$ has four normal modes of vibration active in the infrared [30]. Octahedral $[AlH_6]^{-3}$ units have two normal modes of vibration infrared-active [30]. The infrared active modes in $[AlH_4]^{-1}$ ion for the $NaAlH_4$ are the asymmetric stretching modes at 1680 cm^{-1} and the bending modes in the region 680-900 cm^{-1} [31]. The infrared active modes in $[AlH_6]^{-3}$ are the stretching modes at 1440 and 1290 cm^{-1} and the bending modes in the region 690-930 cm^{-1} [30,31]. Fig. 4b presents the infrared spectra of the hydrogenated materials under different conditions. The region of the bending modes does not properly differentiate between the tetrahedral $[AlH_4]^-$ and octahedral $[AlH_6]^{-3}$ units. The stretching modes are more effective differentiating the tetrahedral $[AlH_4]^-$ and octahedral $[AlH_6]^{-3}$ units. Fig. 4b demonstrated that the hydrided products are a mixture of $NaAlH_4$ and Na_3AlH_6. However, the hydrided material at 100 bar and 200 °C presents a more prominent peak of Na_3AlH_6 (Al–H stretching $[AlH_6]^{-3}$). Meanwhile, the material hydrogenated at 100 bar and 100 °C present the distinctive Al–H stretching peak of $NaAlH_4$ almost of the same intensity of the Al–H stretching $[AlH_6]^{-3}$ peak. X-ray diffraction patterns of the hydrogenated materials confirm the findings of the FT-IR characterization. The hydrided materials are a mixture of Na_3AlH_6, $NaAlH_4$ and Al (in excess). The material hydrided at 100 bar and 100 °C is dominated by the presence of $NaAlH_4$. Meanwhile, the presence of Na_3AlH_6 is more evident in the material hydrided at 100 bar and 200 °C.

Discussion

Despite the apparent simplicity of the described process for recycling Al, the mechanical milling of Al is not a simple process. Normally Al has the tendency of sintering instead of dispersing unless using proper milling conditions [18]. In this work, the milling conditions, particularly the milling time can be considered as not intensive. This is especially important if an industrial application is intended. Furthermore, the ball-milling process of all the precursors of $NaAlH_4$, i.e. the Al_{cans}/NaH/TiF_3/C-nanotubes mixture can be performed in a single step. This also could be of interest for a practical application. All the elements present in the Al from cans, i.e., Mg, Si, Ti, Mn, Fe, Cu, had been used as catalyst in different materials for hydrogen storage. The presence of all this impurities can be beneficial to produce $NaAlH_4$. On the other hand, the purity of materials, and the excess of Al reduced the capacity of hydrogen storage. However, the stored hydrogen of about 3.7 wt % is in the range of other reported materials using high-purity precursors and high-pressure testing [4,5,8,17,28]. An optimization of the additives and the hydrogenation/dehydrogenation conditions is desirable for a practical application.

Although some of the hydrogenation/dehydrogenation conditions were not optimized, the use of recycled aluminum from beverage cans for producing a hydrogen storage material is feasible. This can be an alternative to the purchasing of Al whenever this is not possible or exploitation of a residue is wanted. Three sustainable factors of production of $NaAlH_4$ from recycled aluminum must be highlighted: i) The recycling

of Al necessary involve a reduction of the energy needed for the production of Al from mining. ii) The mechanical-milling process described in the present work can be considered as low-energy consumption due to the process does not involve the melting of Al (high-temperature process). iii) The recycling and the production of the mixture precursor of $NaAlH_4$ are performed in a single step. Thus, the $NaAlH_4$ produced here can be classified as sustainable in addition to contributing to the use of hydrogen as combustible.

Conclusions

A procedure for recycling Al from soft beverage cans to obtain $NaAlH_4$ as a hydrogen storage material was presented. The procedure is simple and easily scalable to industrial applications. Hydrogenation/dehydrogenation experiments demonstrated a reversible storage of 3.7 wt %. This value of hydrogen storage is competitive with $NaAlH_4$ produced from high-purity materials.

Acknowledgment

The present work was supported by the UNAM-DGAPA-PAPIIT IA100817 Estudio del comportamiento masivo de $NaAlH_4$ como material de almacenamiento de hidrógeno obtenido a partir de Al reciclado. Authors thank to Dr. Orlando Hernández for SEM characterization.

Appendix A. Supplementary data

Supplementary data to this article can be found online at https://doi.org/10.1016/j.ijhydene.2019.06.033.

REFERENCES

[1] Rifkin J. The Hydrogen Economy. The creation of the worldwide energy web and the redistribution of power on earth. New York: Penguin Putnam, Inc.; 2007.
[2] Tanç B, Arat HT, Baltacıoğlu E, Aydın A. Overview of the next quarter century vision of hydrogen fuel cell electric vehicles. Int J Hydrogen Energy 2019;44:10120–8. https://doi.org/10.1016/j.ijhydene.2018.10.112.
[3] Moriarty P, Honnery D. Prospects for hydrogen as a transport fuel. Int J Hydrogen Energy 2019;44:16029–37. https://doi.org/10.1016/j.ijhydene.2019.04.278.
[4] Bogdanović B, Schwickardi M. Ti-doped alkali metal aluminium hydrides as potential novel reversible hydrogen storage materials. J Alloy Comp 1997;253–254:1–9. https://doi.org/10.1016/S0925-8388(96)03049-6.
[5] Sakintuna B, Lamari-Darkrim F, Hirscher M. Metal hydride materials for solid hydrogen storage: a review. Int J Hydrogen Energy 2007;32:1121–40. https://doi.org/10.1016/j.ijhydene.2006.11.022.
[6] Paskevicius M, Filsø U, Karimi F, Puszkiel J, Pranzas PK, Pistidda C, et al. Cyclic stability and structure of nanoconfined Ti-doped $NaAlH_4$. Int J Hydrogen Energy 2016;41:4159–67. https://doi.org/10.1016/j.ijhydene.2015.12.185.
[7] Rosli RE, Sulong AB, Daud WRW, Zulkifley MA, Husaini T, Rosli MI, et al. A review of high-temperature proton exchange membrane fuel cell (HT-PEMFC) system. Int J Hydrogen Energy 2017;42:9293–314. https://doi.org/10.1016/j.ijhydene.2016.06.211.
[8] Srinivasan SS, Brinks HW, Hauback BC, Sun D, Jensen CM. Long term cycling behavior of titanium doped $NaAlH_4$ prepared through solvent mediated milling of NaH and Al with titanium dopant precursors. J Alloy Comp 2004;377:283–9. https://doi.org/10.1016/j.jallcom.2004.01.044.
[9] Nielsen TK, Javadian P, Polanski M, Besenbacher F, Bystrzycki J, Skibsted J, et al. Nanoconfined $NaAlH_4$: prolific effects from increased surface area and pore volume. Nanoscale 2014;6:599–607. https://doi.org/10.1039/c3nr03538g.
[10] Nielsen TK, Besenbacher F, Jensen TR. Nanoconfined hydrides for energy storage. Nanoscale 3 2011:2086–98. https://doi.org/10.1039/c0nr00725k.
[11] Carr CL, Jayawardana W, Zou H, White JL, Gabaly FL, Conradi MS, et al. Anomalous H_2 desorption rate of $NaAlH_4$ confined in nitrogen-doped nanoporous carbon frameworks. Chem Mater 2018;30:2930–8. https://doi.org/10.1021/acs.chemmater.8b00305.
[12] Sanjeev L. Process for preparing dry sodium aluminum hydride. U.S. Patent No. 5 1994. 295,581, 22.03.
[13] Gross K, Majzoub E. Direct synthesis of catalyzed hydride compounds. U.S. Patent No. US2003 0143154 A1; 2003.
[14] Huot J, Ravnsbæk DB, Zhang J, Cuevas F, Latroche M, Jensen TR. Mechanochemical synthesis of hydrogen storage materials. Prog Mater Sci 2013;58:30–75. https://doi.org/10.1016/j.pmatsci.2012.07.001.
[15] Xiao XZ, Chen LX, Fan XL, Wang XH, Chen CP, Lei YQ, et al. Direct synthesis of nanocrystalline $NaAlH_4$ complex hydride for hydrogen storage. Appl Phys Lett 2009;94. 041907-3, https://doi.org/10.1063/1.3076104.
[16] Fan X, Xiao X, Chen L, Yu K, Wu Z, Li S, et al. Active species of $CeAl_4$ in the $CeCl_3$-doped sodium aluminium hydride and its enhancement on reversible hydrogen storage performance. Chem Commun 2009:6857–9. https://doi.org/10.1039/B916898B.
[17] Bergemann N, Pistidda C, Milanese C, Girella A, Hanse BRS, Wurr J, et al. $NaAlH_4$ production from waste aluminum by reactive ball milling. Int J Hydrogen Energy 2014;39:9877–82. https://doi.org/10.1016/j.ijhydene.2014.02.025.
[18] Prieto-Martínez V, Torres-Torres J, Flores-Valdés A. Recycling of aluminum beverage cans for metallic foams manufacturing. J Porous Mater 2017;24:707–12. https://doi.org/10.1007/s10934-016-0307-8.
[19] Nunes R. ASM Handbook volume 2: properties and selection: nonferrous alloys and special purpose materials. ASM International; 1990.
[20] Fan X, Xiao X, Chen L, Li S, Ge H, Wang Q. Enhanced hydriding-dehydriding performance of $CeAl_2$-doped $NaAlH_4$ and the evolvement of Ce-containing species in the cycling. J Phys Chem C 2011;115:2537–43. https://doi.org/10.1021/jp1089382.
[21] Fan X, Xiao X, Chen L, Han L, Li S, Ge H, et al. Hydriding-dehydriding kinetics and the microstructure of La- and Sm-doped $NaAlH_4$ prepared via direct synthesis method. Int J Hydrogen Energy 2011;36:10861–9.
[22] Ramezani M, Neitzert TJ. Mechanical milling of aluminum powder using planetary ball milling process. Achiev Mater Manuf Eng 2012;55:790–8. https://pdfs.semanticscholar.org/6f79/315584ec12dd1d6fb0a8a2badb1de35f8e5f.pdf.
[23] Dehouche Z, Lafi L, Grimard N, Goyette J, Chahine R. The catalytic effect of single-wall carbon nanotubes on the hydrogen sorption properties of sodium alanates. Nanotechnology 2005;16:402–9. https://iopscience.iop.org/article/10.1088/0957-4484/16/4/012/meta.

[24] Chen TT, Yang CH, Tsai WT. In-situ synchrotron X-ray diffraction study on the dehydrogenation behavior of $NaAlH_4$ modified by multi-walled carbon nanotubes. Int J Hydrogen Energy 2012;37:14285–91. https://doi.org/10.1016/j.ijhydene.2012.07.012.

[25] Carrillo-Bucio JL, Tena-Garcia JR, Armenta-Garcia EP, Hernandez-Silva O, Cabañas-Moreno JG, Suárez-Alcántara K. Low-cost Sieverts-type apparatus for the study of hydriding/dehydriding reactions. HardwereX 2018;4. e00036-14, https://doi.org/10.1016/j.ohx.2018.e00036.

[26] Léon A, Kircher O, Rösner H, Décamps B, Leroy E, Fichtner M, Percheron-Guégan A. SEM and TEM characterization of sodium alanate doped with $TiCl_3$ or small Ti clusters (Ti_{13}*6THF). J Alloy Comp 2006;414:190–203. https://doi.org/10.1016/j.jallcom.2005.04.212.

[27] Bogdanović B, Brand RA, Marjanović A, Schwickardi M, Tölle J. Metal-doped sodium aluminium hydrides as potential new hydrogen storage materials. J Alloy Comp 2000;302:36–58. https://doi.org/10.1016/S0925-8388(99)00663-5.

[28] Lozano GA, Ranong CN, Bellosta von Colbe JM, Bormann R, Fieg G, Hapke J, et al. Empirical kinetic model of sodium alanate reacting system (I). Hydrogen absorption. Int J Hydrogen Energy 2010;35:6763–72. https://doi.org/10.1016/j.ijhydene.2010.04.080.

[29] Lozano GA, Ranong CN, Bellosta von Colbe JM, Bormann R, Fieg G, Hapke J, et al. Empirical kinetic model of sodium alanate reacting system (II). Hydrogen desorption. Int J Hydrogen Energy 2010;35:7539–46. https://doi.org/10.1016/j.ijhydene.2010.04.142.

[30] Nakamoto K. Infrared and Raman spectra of inorganic and coordination compounds. Part A: theory and applications in inorganic chemistry. New Yersey: John Wiley & Sons, Inc.; 2009.

[31] Tsumuraya T, Shishidou T, Oguchi T. *Ab initio* study on the electronic structure and vibration modes of alkali and alkaline-earth amides and alanates. J Phys: Condens Matter 2009;21:185501–9. https://doi.org/10.1088/0953-8984/21/18/185501.

[32] Qiu C, Opalka SM, Olson GB, Anton DL. Thermodynamic modeling of the sodium alanates and the Na-Al-H system. Int J Mat Res 2006;97:1484–94. https://doi.org/10.3139/146.101410.